# Sediment properties influencing upwelling spectral reflectance signatures: The "biofilm gel effect"

*Alan W. Decho and Tomohiro Kawaguchi*

Department of Environmental Health Sciences, Norman J. Arnold School of Public Health, University of South Carolina, Columbia, South Carolina 29208

*Mead A. Allison*

Department of Geology, Tulane University, New Orleans, Louisiana 70118

*Eric M. Louchard and R. Pamela Reid*

Marine Geology and Geophysics, RSMAS, University of Miami, 4600 Rickenbacker Causeway, Miami, Florida 33149

*F. Carol Stephens*

Marine Biology and Fisheries, RSMAS, University of Miami, 4600 Rickenbacker Causeway, Miami, Florida 33149

*Kenneth J. Voss*

Department of Physics, University of Miami, Coral Gables, Florida 33124

*Robert A. Wheatcroft*

College of Oceanic and Atmospheric Sciences, Oregon State University, Corvallis, Oregon 97331

*Brenton B. Taylor*

Department of Oceanography, Texas A&M University, 5007 Ave. U., Galveston, Texas 77551

*Abstract*

   Microbial communities often produce copious films of extracellular polymeric secretions (EPS) that may interact with sediments to influence spectral reflectance signatures of shallow marine sediments. We examined EPS associated with microbial mats to determine their potential effects on sediment reflectance properties. Distinct changes in spectral reflectance signatures of carbonate sediments from the Bahamas were observed among several sediment sites, which were specifically chosen for their presence of microbial mats and adjacent nonmat sediments. The presence of mats greatly reduced sediment reflectance signatures by $\sim$10%–20%, compared with adjacent nonmat areas having similar sediment characteristics. Decreases in reflectance near 444 and 678 nm could be attributed primarily to absorbance by photopigments. However, additional nonspecific decreases in reflectance occurred across a wide spectral range (400–750 nm). Experimental manipulations determined that nonspecific reflectance decreases were due to EPS that are produced by biofilm-associated microorganisms of the mats. Microbial EPS, isolated from natural mat sediments exhibited small but nonspecific absorbances across a broad spectral range. When EPS was in relatively high concentrations, as in microbial mats, there was a "biofilm gel effect" on sediment reflectance properties. The effect was twofold. First, it increased the relative spacing of sediment grains, a process that permitted light to penetrate deeper into sediments. Second, it resulted in a more efficient capture of photons because of the change in refractive index of EPS gel itself relative to seawater. The relatively translucent EPS of biofilms, therefore, influenced the magnitude of reflectance across a broad spectral range in marine sediments.

   Downwelling light, on interaction with carbonate sediments, produces variable upwelling reflectance and scatter-

ing signature (Mobley 1994). The upwelling signatures result from absorption, scattering, and reflectance interactions with sediment properties that may vary over a range of different spatial scales (e.g., km to $\mu$m). For example, small-scale (cm to m) changes in sediment topography resulting from disturbances by storms or animal burrowing activities may potentially influence reflectance spectra (Serodio et al. 1997). The presence/absence of microbial mats may effect spectral changes that are detectable at much larger scales (Philpot 1989; Paterson et al. 1998; Yates et al. 1993). The spectral changes, detectable at many spatial scales, ultimate-

ly result from photon interactions occurring because of fine-scale features of sediments. Therefore, an understanding of how light interacts with marine sediments requires examination of smaller scale features of sediment systems.

The fine-scale features of a sediment surface may act as a potential "optical filter," affecting the inherent optical properties of sediments. The fine-scale features may vary depending on specific biological, chemical, and geological properties of sediments. Geological features such as mineral composition, grain size, and shape may influence spectral reflectance signatures. For example, sediment grain size and shape influences the interstitial pore space of sediments and hence may affect the ability of light to enter into or be scattered off of the sediment surface. Larger sediment grains sizes will generally result in larger interstitial pores and a deeper depth penetration of light, all else being constant. Chemical features of sediments, such as the presence of humic organic matter coatings or precipitates on sediment particle surfaces, may also influence spectral reflectance signatures.

The fine-scale microstructure of sediments can be altered by the presence of microbial biofilms or larger scale microbial mats (Paterson 1995). They form coatings on the surfaces of sediment particles or may collectively form larger structured microbial mats that extend meters across the sediment surface. Biofilms consist of microbial cells (nonphotosynthetic and photosynthetic bacteria and microalgae) embedded within a secreted matrix of extracellular polymers (Costerton et al. 1995). Earlier work by Amos et al. (1996) and Sutherland (1996) documented changes in the bulk density of surface (i.e., top 1.5 mm) sediments, relative to deeper sediments. De Winder and Stal (1997), using resistivity measurements, showed that there was increased porosity in the surface 500 $\mu$m of sediment associated with mats. With the application of low-temperature scanning electron microscopy the fine-scale features of sediments, while in a hydrated state, could be examined. Using a rapid-freezing technique that minimized sample distortion artifacts, Paterson et al. (1998) observed surfaces of mudflat sediments and found an abundance of extracellular polymeric secretions (EPS) in the surface of the mats. They noted that the vertical migratory patterns of microphytobenthos occurring over a tidal cycle influenced the reflectance signatures of surface sediments. They also showed that grain spacing, cell numbers, and other sediment properties varied over relatively small spatial scales (i.e., $\mu$m to mm). The studies suggested that the presence of microbial communities and their EPS significantly alter the surface fabric of sediments, a property that may influence optical signatures of sediments.

The biofilm will contain a concentrated array of cells and their associated pigments and large polymeric molecules (Decho 1990), all of which affect potential absorption, scattering and reflectance. In addition, vertical migrations of microbial cells (e.g., diatoms) within a biofilm may occur quite rapidly (Hay et al. 1993), changing the observable pigment-related optical spectra of surface sediments. The presence of dense gels of EPS, secreted by the biofilm community, may also influence the relative spacing of sediment grains and influence relative porosity of surface sediments.

Previous studies determined that the presence of microbial mats influence the light transmission and reflectance properties of sediments (Lassen et al. 1992; Kühl et al. 1994*a*; Paterson et al. 1998). Our preliminary observations (unpubl. data) suggested that sediment samples containing abundant microbial biofilms (and EPS) had a lower reflectance than similar sediments containing less biofilm material. We hypothesized that the changes in spectral reflectance may be due, in part, to the EPS matrix that is abundantly present in microbial mats. Our study, therefore, focused on how the biofilm EPS matrix may alter the optical properties of sediments through changes in absorption, scattering and reflectance.

## Materials and Methods

*Sediment sites and collection of natural sediment samples*—All field work was conducted at the Caribbean Marine Research Center (CMRC), located at Lee Stocking Island (LSI) in the Exumas, Bahamas. Sediment samples were collected from three sites in proximity to CMRC: (1) North Perry Reef (NP; 23°46.98′N, 76°6.05′W; 17–20 m depth); (2) Twin Beaches (TB; 23°45.57′N, 76°5.52′W; ~2 m depth), which is a shallow-water site and contains abundant diatom mats; and (3) Ooid Shoals (OS; 23°45.65′N, 76°6.77′W; depth 1.0–1.5 m). This site contained relatively well-sorted carbonate ooids (100–300 $\mu$m) and had a low (<0.1%) organic matter content. The NP and TB sites were selected because they contained abundant microbial biofilm mats that were designated as "mat" sediments, with adjacent patches of sediment containing no noticeable microbial mats, designated as "no mat" sediments. The OS site was chosen for apparent lack of biofilm mats and represented a relatively clean sand site. High currents and ooid sand bedforms occurred at the OS site. Some ooids from this site are likely colonized by endolithic cyanobacteria, because exolithic forms would have been scoured from sediment particles by bed-load transport at this high-energy site. The endolithic cyanobacteria were detectable via spectral reflectance and resulted in a minimal pigment signature.

Natural sediment samples were collected by SCUBA using transparent plastic coring tubes (2.2 × 10 cm). All samples were collected near midday, during high ambient light conditions. The cores were vertically inserted into sediments within a 0.25 m² grid at each study site for measurement of hyperspectral reflectance at the surface of the cores and for pigment analyses by high-performance liquid chromatography (HPLC). Cores were returned to the laboratory at LSI, where reflectance measurements were made. This technique allowed the surface microbial film and sediments to remain relatively undisturbed. The sediment cores and their overlying water were transported back to the laboratory. Reflectance measurements were made within 6 h after collection. After completion of the reflectance measurements, the upper 5 mm of each core was removed and frozen in liquid nitrogen for photosynthetic and photoprotective pigment analyses. The upper 5 mm of additional cores was used for determination of dry bulk density. Certain analytical measurements required disruption or destruction of samples; therefore, the same replicate samples could not be used for

all measurements. Reflectance measurements were conducted on the same samples used for pigment analyses (by HPLC). Sediment porosity and light penetration measurements were conducted on the same samples. EPS, scattering, and grain-size analyses were conducted on separate samples.

*Isolation and purification of natural EPS from sediments*—Natural EPS were extracted from sediments for later analyses. Triplicate samples were used for each measurement. From each sample, the uppermost (5 mm) surface layer of sediments was collected and placed into a glass vial. EPS material was initially extracted by mixing mat material with ethylene diaminetetraacetic acid (EDTA; in seawater, final concentration of 4 mM) and gentle heating to 40 ± 1°C for 15 min, with occasional stirring. Samples were lightly homogenized to separate sand grains using a blunt plastic probe. The solubilization of EPS did not lyse cyanobacteria, dinoflagellates, or diatom cells. The suspension, containing cells, detritus, and EPS, was placed in microfuge tubes and centrifuged (10,000 × g, 6 min) to pelletize cells and particulate detritus. The resulting supernatant, containing EPS, was removed by pipette, mixed with 70% (final concentration) cold (4°C) ethanol, and precipitated for 8 h. The pellet and remaining sediment were reextracted using EDTA and heating as described above. This latter procedure was performed three times, for a total of four extractions. Preliminary experiments showed no detectable EPS after three extractions. Precipitated material from the supernatant was collected by centrifugation, then redissolved in deionized H₂O. The ethanol precipitation was repeated twice, then the EPS was dialyzed (12,000 molecular weight cutoff) against several changes of deionized H₂O for 24 h. EPS was lyophilized to dryness, then stored at −70°C prior to analysis. The sediments from each sample were washed with deionized H₂O to remove salts and loosely bound detritus, then dried for determination of dry weight. All EPS concentrations were normalized to sediment dry weight. Quantification of EPS material was conducted using two methods: the phenol-sulfuric acid method (Dubois et al. 1956; Underwood et al. 1995; Smith and Underwood 1998) and by total EPS dry weight. D-glucose and alginic acid were used as reference standards for the spectrophotometric determinations.

*Spectral absorbance properties of EPS*—Purified EPS samples, extracted from natural sediment biofilms, were analyzed by UV-VIS spectroscopy to obtain absorption spectra (250–700 nm). EPS absorption efficiency factors were examined at 0.5%, 1.0%, 2.0%, and 4.0% (wt/vol) in 30 g L⁻¹ artificial seawater, using seawater as a reference. Artificial seawater was prepared by adding the following components to deionized water: 460 mmol L⁻¹ NaCl, 55 mmol L⁻¹ MgCl₂·6H₂O, 11 mmol L⁻¹ CaCl₂·2H₂O, 10 mmol L⁻¹ KCl, and 2.5 mmol L⁻¹ NaHCO₃. Absorption efficiency spectra were measured using a UV-2401 PC spectrophotometer system (Shimadzu Scientific Instruments). Calculation of molar absorptivity (molar extinction coefficient) of EPS was based on an estimated molecular weight of 100 kDa and a 0.4 mmol L⁻¹ concentration (4% wt/vol), according to the equation

$$\varepsilon = A(C \times l)^{-1} \qquad (1)$$

where $\varepsilon$ = absorption coefficient ([mol L⁻¹]⁻¹ cm⁻¹); $A$ = absorbance; $C$ = molar concentration (mol L⁻¹); l = path length (cm).

*Nanoplast embedding and confocal scanning laser microscopy*—Fluorescent probes were used to image the microspatial arrangements of microbial cells, ooids, and EPS in samples of mat and no-mat sediments from the samples sites. "High ALG-SED" (i.e., containing added EPS) and "clean-SED" sediments (i.e., containing no added EPS) were used in the laboratory reflectance experiments (described below). The following fluorescent probes were used: propidium iodide and/or 4,6-damidino-2-phenyl-indole to label bacteria cells, fluorescein isothiocyanate (FITC)–concanavalin A to label EPS, and autofluorescence to image ooids and CaCO₃ precipitates. Freshly collected samples were sectioned using sterile razor blades. Immediately after collection, the sections of sediment were preserved in EM–grade 3% formaldehyde (in seawater). The sections were incubated in different fluorescent probes for 1 h (Decho and Kawaguchi 1999, 2000). After the incubations, unbound probes were removed by washing 3 times with 20 ml sterile-filtered seawater for 10 min each. Excess water was gently removed using glass pipettes. The samples were then embedded in hydrophilic Nanoplast embedding resin over several days. according to the methods described in Decho and Kawaguchi (2000). Embedded samples were thick-sectioned (1 mm) and mounted on glass microscope slides. A cover slip was mounted on samples on glass slides with a Epon mounting solution. Samples were viewed under MRC 1024MP confocal scanning laser microscopy system (Bio-Rad Laboratories) equipped with an Eclipse TE 300 compound-inverted microscope (Nikon).

For experimental laboratory sediment studies using alginate, EPS were imaged by biotinylation of carboxyl groups (on uronic acids) using the EZ-Link 5-(biotinamido) pentylamine (Pierce). FITC conjugated to streptavidin (1 : 100) in phosphate-buffered saline (PBS), was applied to biotinylated alginate, then incubated at room temperature for 1 h and washed in PBS three times. FITC-labeled alginate could then be observed using confocal scanning laser microscopy.

*Spectral reflectance measurements*—Laboratory experiments were conducted to determine how the presence of EPS on sediments might influence the spectral reflectance of sediments. Hyperspectral reflectance was measured by placing a core tube containing sediment covered by seawater in a custom-built polyvinyl carbonate (PVC) holder designed to exclude ambient light. A reflectance probe (Ocean Optics RP200-7) was inserted into the top of the core holder so that the probe tip was underwater, 25 mm from and oriented 0° to the sediment surface. An Ocean Optics S2000 UV-VIS spectrometer (grating #3), with 2,048 channels (dispersion, 0.32 nm pixel⁻¹; optical resolution, 2.06 nm) was connected to the RP200-7 by a 200 µm fiber-optic cable and cojoined to an Ocean Optics LS-1 tungsten halogen light source. Reflectance of a diffuse reflectance WS-1 Spectralon standard (99% reflective) (Labspere) was measured in a PVC cylinder

filled with filtered seawater that was similar in design to the one used for the core measurements. Counts were measured in the dark to account for dark current noise of the instrument. Integration times over which the measurements were made were varied to obtain a maximum signal-to-noise ratio without saturating the spectrometer. Radiance reflectance ($R$) was calculated as the ratio of the counts measured on the sample divided by the counts measured on a calibrated Spectralon diffuse reflectance standard and then multiplied by the calibration factor (0.99) for the Spectralon standard as follows:

$$R = (C^l - C^d/CS^l - CS^d)/(int^s/int) \times 0.99 \quad (2)$$

where $C^l$ is the spectrometer count of the sample, $C^d$ is the dark-current count for the sample, int is integration time for the sample, $CS^l$ is the spectrometer count of the standard, $CS^d$ is the dark-current count for the standard, and $int^s$ is the integration time for the standard.

The WS-1 standard was held in a PVC cylinder similar to the cylinder used for the sediment cores, with the RP200-7 probe clamped at a constant 25-mm distance normal to the WS-1 surface. Reflectance measurements for the WS-1 standard were made 10 times with the light source on and 10 times with the light off for the dark-current measurement. Replicate samples of intact natural sediments from each site were collected, as described above, and returned to the laboratory and analyzed using the same reflectance procedure.

*Manipulation experiments using artificial EPS-coated sediments*—Sediments used in laboratory reflectance experiments were carbonate ooids, collected from the "Channel Marker" site (23°45.65′N, 76°6.77′W). This site contained relatively well-sorted carbonate ooids (100–300 $\mu$m) and had a low amount (<0.1%) of organic matter present, although endolithic cyanobacteria were detectable within ooids and resulted in a minimal pigment signature. Ooids were returned to the laboratory, sieved through a 250-$\mu$m screen to remove larger grains, then placed in sodium hypochlorite (24 h) to oxidize most of the organic matter. The ooids were extensively rinsed and soaked in distilled H$_2$O, then dried and stored. These ooids were designated as "clean-SED." Alginate (Na-salt alginic acid; Sigma-Aldrich) was used as an artificial EPS for laboratory experiments. Alginate consists of two uronic acid monomers, guluronate and mannuronate. Because this polymer contains abundant carboxyl groups, additions of Ca$^{2+}$ ions result in a very homogeneous mucous gel. This property was used to construct sediment treatments. Clean-SED were coated using two different concentrations (2% and 4% wt/vol) of alginate. Coatings on sediments were obtained by first fully dissolving alginate in deionized water (18 M$\Omega$ resistance). This formed a viscous solution. Then a preweighed amount (10 g) of clean sediments was added to the alginate (5 Ml). The alginate-sediment mixtures were carefully added as a surface layer to the cores. Finally, filtered seawater was added to the sediment-polymer mixture and incubated for 2–3 h. The sediment polymer mixtures rapidly formed gels. Sediment reflectance measurements were conducted in the plexiglass core tubes (see above). To prepare a sediment core, clean-SED was added to the core tube to a specified height, then

sediment from one of three treatments ("clean-SED," "low-ALG SED" [2%], or "high ALG-SED" [4%]; see above) was added by pipette as a separate layer (~0.5 cm thick) on top of the sediments. Care was taken to make sure that the sediment treatment layers were as homogeneous as was possible.

*HPLC pigment analyses*—Pigment fingerprinting was conducted to measure the relative amounts of chlorophylls *a* and *b* and accessory pigments as a conservative indication of major photosynthetic groups in mat and no-mat areas. Chlorophyll and carotenoid pigments were extracted from the sediment samples with 100% acetone (−10°C) by sonication in an ice bath for 1 min in 15-s bursts. Pigment extraction was allowed to continue for 24 h in a freezer at −10°C, after which the samples were mixed thoroughly with a vortex mixer and allowed to settle for at least 1 h before analysis. Pigment analysis was conducted with a Hewlett Packard 1100 series high-performance liquid chromatograph equipped with a diode array detector. The method used was similar to that of Van Heukelem et al. (1994), with columns maintained at 35°C. However, as suggested by Pinckney et al. (1996), three C$_{18}$ columns were used in series to enhance pigment separation. The first column was a Rainin monomeric Microsorb-MV column, 0.46 × 10 cm, 3 $\mu$m packing, followed by two polymeric Vydac 201TP columns, 0.46 × 25 cm, 5 $\mu$m packing. A binary solvent system was used with solvent A (methanol : 0.5 M ammonium acetate, 80 : 20) and solvent B (methanol : acetone, 80 : 20) to separate pigments. Identification and quantification of pigments was made by comparing retention times and peak areas with pigment standards obtained from VKI Water Quality Institute (Agern Alle ll, DK-2970 Hørsholm). Pigment peak identifications and purity were confirmed with the diode array detector. On completion of the pigment analyses, extracted sediment was rinsed with distilled water and dried in a 90°C oven for dry-weight determination. Individual pigment concentrations were then calculated relative to dry weight of each sample and then multiplied by bulk dry density to yield $\mu$g pigment cm$^{-3}$.

*Scattering and refractive index measurements*—The EPS matrix may alter the scattering of light entering a mat. Therefore, we examined the effect of EPS on the forward-scattering, relative to back-scattering of photons. The bidirectional reflectance distribution function (BRDF) was measured with the BRDF meter (Voss et al. 2000) for the TB site (mat and no-mat) and the OS site. Because the sediments at the TB site were softer, the measurement procedure included taking a core sample. A 10-cm diameter two-part Plexiglas/plastic tube was used to obtain core samples of the two types of sediments (clear tubing on top, opaque tubing on the bottom). The cores were obtained by pressing these large diameter tubes into the sediment, normal to the surface. The tubes were pressed into the surface until the sediment was level with the division between the two types of tubing. A cover was placed over the top of the sampler, and a second cover was slid under the sampler. The core sample was placed in a measurement stand (in situ, next to the core site and submerged) and the clear portion removed, leaving a

Table 1. Sampling site characteristics of mat and no-mat areas of three sediment sites.

| Site | Description | Mean grain size ($\mu$m $\pm$ SE) |
|---|---|---|
| Twin Beaches: mat | Shallow (1.5 m) near-shore area with low current near seagrass beds. | 354$\pm$156 |
| Twin Beaches: no-mat | Shrimp mound in shallow (1.5 m) nearshore area. | 203$\pm$331 |
| North Perry | | |
| Mat | Sediment with thick algal layer in deep (16 m) area near coral reef. | 649$\pm$330 |
| No-mat | Bioturbated patches of sediment in deep (16 m) area near coral reef. | 574$\pm$356 |
| Ooid Shoals | Migrating ooid shoal in a channel between islands | 430$\pm$349 |

sample that was level with the instrument stand. The BRDF instrument was then placed on this stand and the BRDF measurement taken. In this way, the weight of the instrument did not compress the sediment in any way, and the height of the sediment relative to the instrument measurement point could be determined precisely. At the OS site, the sediment was more uniform and could easily support the weight of the instrument. Thus, the BRDF meter was placed directly on the sediment.

The refractive index (RI) of the alginate gel (4%) was determined by measuring the angular deviation of a laser beam when entering a gel sample. The gel was made in 1-cm-square cuvettes. A laser beam was directed at the cuvette at different incident angles, ranging from 30 to 60°. The angular deviation of the laser beam when transiting the gel was measured, and the RI was determined using Snell's law. The measurements were duplicated with freshwater in the cuvettes for comparison.

*Measurement of light penetration into sediments*—Light penetration into the sediments (and laboratory samples) was measured with fiber-optic microprobes. The purpose was to determine how the presence of mats (and more specifically their EPS) influenced the downward penetration of light. Probes were constructed with 200 $\mu$m UV/VIS optical fibers encased in a stainless steel syringe of 450 $\mu$m diameter. The tip of the fibers was ground flat to produce a diffuse (in air) cosine collector. Spectral measurements from 400–1,000 nm were made with an S2000 Ocean Optics spectrometer. Probes were inserted downward (to measure upwelling light) into sediment cores collected within a 24-h period of the experiment. Cores contained intact stratigraphy and overlying water. Overhead light (~10° from the vertical) was provided with a collimated quartz-halogen source. Measurements were made at 100 $\mu$m depth intervals using a micrometer-based insertion system. All data were ratioed to light levels measured at the sediment surface. Several experiments were also conducted with probes inserted from below to determine the comparability of upwelling versus downwelling values.

*Sediment porosity*—Porosity was examined to understand how the presence of EPS may influence grain spacing near

the sediment surface. Measurements of porosity were made using a newly developed in situ resistivity profiler (described by Wheatcroft in press). In brief, the system is a four-electrode probe that is pushed into the seafloor by a motor coupled to a lead screw. The profiler logs sediment resistivity at 0.25-mm depth intervals over the upper 10–15 cm of the seabed. Divers can position the profiler over seafloor features of interest; for example, ripple crests or microalgal mats, before initiating a profile. Porosity is estimated from resistivity using the well-known Archie's (1942) relationship, $F = \phi^m$, where $F$ is the formation factor (the measured ratio of bottom water to sediment resistivity), $\phi$ is the porosity and $m$ is an empirical constant. Laboratory and field techniques were used to determine $m$ for each of the study sites (Wheatcroft in press).

## Results

*Sampling sites*—Three sediment sites, NP, TB, and OS, were used in this study. The first two sites were characterized by meter-sized patches of microbial mats and adjacent patches of barren sand (i.e., no-mat) that were easily visible using SCUBA. The surface sediments of mat areas at the North Perry site contained a thick cohesive biofilm that was patchy even within the 0.25 m$^2$ grid within which replicate cores were collected. The third site, OS, contained relatively "clean" sand, with no noticeable accumulations of mat or other organics. Grain-size distributions for the three sites are listed in Table 1.

*EPS abundance*—The highest EPS abundance (274 $\mu$g EPS g$^{-1}$ sediment) occurred at mat areas of the TB site. At both the NP and TB sites, EPS abundance were ~10–20-fold higher in mat areas, compared with adjacent no-mat areas (Fig. 1). The mean ($\pm$SE) hexose-equivalent (polysaccharide) content of EPS isolated from mat sediments, as measured by the phenol-sulfuric acid method, was 33 $\pm$ 1.1% ($n = 3$; wt%) and 11.2 $\pm$ 1.1% ($n = 3$) at no-mat areas of the TB site. NP mat sediments had a mean hexose equivalent content of 13.7 $\pm$ 0.9% ($n = 3$), whereas contents in no-mat areas were below detection limits.
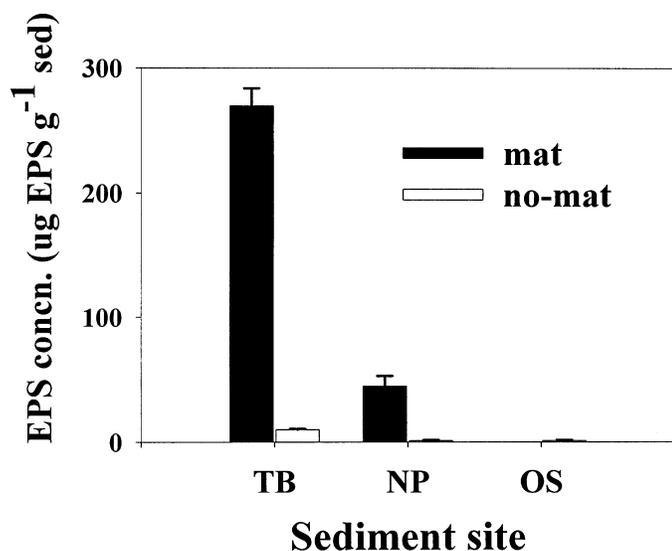
Fig. 1. Mean ($\pm$SE; $n = 3$) concentrations of EPS in sediments of mat and no-mat areas at three sample sites. EPS abundance is $\mu$g EPS g$^{-1}$ sediment.



Fig. 2. Absorbance spectra of natural and laboratory EPS. Natural EPS was isolated from mat areas of TB and NP. Laboratory EPS was sodium alginate. Absorbance units ($y$-axis) are relative to seawater blank. All spectra were determined at a concentration of 4 wt%.

*Spectral absorbance*—Absorption by EPS over a wide spectral range (250–700 nm) was relatively low (Fig. 2). Spectral absorption by EPS over most of the visible light spectrum (i.e., 400–700 nm) showed a wavelength-dependent absorbance pattern, with increasing absorption at decreasing wavelengths. Molar extinction coefficients, calculated at the peak absorbance wavelengths of Chl *a* pigment (i.e., 444 and 678 nm) were 7,742 and 7,192 (mol L$^{-1}$)$^{-1}$ cm$^{-1}$, respectively. Absorption increased in a concentration-dependent manner, over the concentration range of most observed EPS (0.5–4.0 wt%).

*Pigments*—Microalgal biomass in ooid sand at the OS site had the lowest content of Chl *a* (2.29 $\mu$g cm$^{-3}$) pigment, compared with all sites. There was a presence of zeaxanthin and echinenone and a lack of Chl *b* and lutein. No-mat area sediments at the TB site contained Chl *a* (0.82 $\mu$g cm$^{-3}$). The sediments contained an almost equal amount of chlo-

rophyllide *a* (0.93 $\mu$g cm$^{-3}$). Fucoxanthin was the most abundant taxonomically significant accessory pigment present in this habitat. Peridinin, zeaxanthin, and echinenone pigments were present in this microalgal community as well. Small amounts of lutein were measured, although Chl *b* was below detection limits. However, the mean Chl *a* content (3.48 $\mu$g cm$^{-3}$) of mat sediments was approximately four times greater than adjacent no-mat sediments. The mat areas of the NP site had Chl *a* concentrations that were approximately five times greater than those at the other study sites. In the no-mat areas, the mean Chl *a* concentration was 9.47 $\mu$g cm$^{-3}$, in contrast to mat areas where the mean Chl *a* concentration was 16.22 $\mu$g cm$^{-3}$. The pigments peridinin, Chl *b,* and lutein and zeaxanthin and echinenone were also present in measurable quantities (Table 2). In contrast to the other study sites, 19'-butanoyloxyfucoxanthin was detected.

*Reflectance spectra*—The surfaces of intact sediment cores of both mat and no-mat sediments exhibited major and

Table 2. Microalgal pigment concentrations in the top 5 mm of sediment cores. ND, not detected; *n*, number of replicate cores analyzed for each site (SE in parentheses).

| Pigment Concentration ($\mu$g cm$^{-3}$ sediment) Mean ($\pm$SE) | Ooid Shoals no-mat ($n = 10$) | Twin Beaches no-mat ($n = 10$) | Twin Beaches mat ($n = 10$) | North Perry no-mat ($n = 3$) | North Perry mat ($n = 16$) |
|---|---|---|---|---|---|
| 19'-Butanoyloxyfucoxanthin | ND | ND | ND | 0.02 (0.01) | 0.07 (0.01) |
| $\beta$-carotene | 0.21 (0.02) | 0.02 (0.01) | 0.10 (0.02) | 0.41 (0.15) | 0.67 (0.07) |
| Chlorophyll *a* | 2.29 (0.64) | 0.82 (0.13) | 3.48 (0.46) | 9.47 (2.98) | 16.22 (1.15) |
| Chlorophyllide *a* | ND | 0.93 (0.17) | 4.12 (0.54) | 0.41 (0.15) | 4.25 (0.69) |
| Chlorophyll *b* | ND | ND | ND | 0.05 (0.05) | 0.13 (0.05) |
| Diadinoxanthin | ND | 0.10 (0.02) | 0.43 (0.06) | 0.41 (0.11) | 0.76 (0.05) |
| Echinenone | 0.08 (0.01) | <0.01 | 0.06 (0.01) | ND | 0.16 (0.02) |
| Fucoxanthin | 0.02 (0.01) | 0.46 (0.08) | 1.60 (0.21) | 4.44 (1.42) | 8.32 (0.49) |
| Lutein | ND | 0.02 (0.01) | 0.03 (0.01) | 0.11 (0.02) | 0.14 (0.03) |
| Peridinin | ND | 0.05 (0.01) | 0.07 (0.01) | 0.06 (0.04) | 0.06 (0.02) |
| Zeaxanthin | 0.32 (0.01) | 0.06 (0.01) | 0.11 (0.01) | 0.28 (0.10) | 0.66 (0.05) |
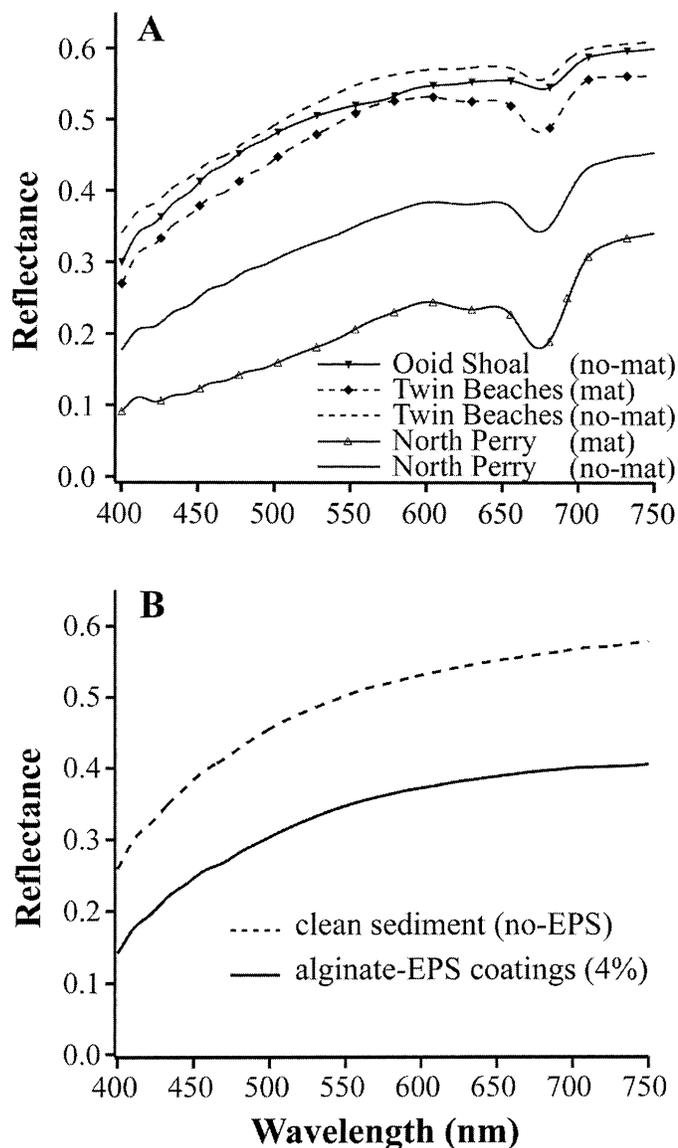
Fig. 3. Spectral reflectance measurements of (A) natural carbonate surface sediments at three sites. Note decreases in magnitude of reflectance lines in mat areas, compared with their no-mat counterparts within a site. (B) Experimental sediments (e.g., "clean" sediments having no added EPS, and sediments having "alginate-EPS coatings") exhibit a similar decrease in reflectance magnitude because of the presence of EPS.

specific decreases in reflectance at both 444 and 678 nm (Fig. 3). Examinations of spectra across a wide spectral range (400–700 nm) revealed that the magnitude of relative reflectance decreased in mat area cores (~15%–20%), compared with cores from adjacent no-mat areas. Reflectance spectra typically varied both in magnitude and shape between sites and areas within a site. Reflectance was highest at the TB site in no-mat sediments and at the OS site. The lowest reflectance measured was at the NP site within mat areas. Laboratory studies of the effect of the EPS itself indicate that the EPS alone on bleached sediments contributed to as much as a ~25% decrease in the magnitude of reflec-

tance from 400 to 710 nm (Fig. 3). The presence of EPS gels also increased the relative spacing of sediment grains.

*Light penetration*—Qualitative examinations using confocal scanning laser microscopy of EPS-laden, mat sediments compared with adjacent no-mat sediments showed a greater relative spacing of sediment grains in mat sites (Fig. 4). The presence of mats was associated with a deeper penetration of light into sediments. At all sites, the depth of light penetration was strongly related to wavelength. In general, longer wavelengths penetrated more deeply in the highly scattering sediment medium (Fig. 5). At a given wavelength, light penetrated to greater depths in mat sediments when compared to no-mat areas. The depth to 10% of incident light of the mat samples was, on average, 28% deeper at TB and 78% at NP compared with no-mat samples from the same site. Penetration depths to 10% incident were similar for no-mat areas from all three sites, ranging from 1.4 to 1.6 mm at 500 nm.

*Changes in scattering and RI*—Sediments having higher EPS concentrations exhibited increased forward scattering, relative to no-mat sediments. The presence of EPS in sediment reduced the relative RI of the grain, compared with a similar grain in seawater. The RI of EPS was 1.40 and was higher compared with seawater (RI = 1.35) and lower compared with ooid grains (RI = 1.55). Experimental results showed that, when embedded within an EPS matrix, the relative RI of an ooid grain was 1.11, rather than 1.15 when in seawater alone. The RI of the EPS was relatively independent of ionic concentration (e.g., $Ca^{++}$ or $Mg^{++}$) (data not shown). Decreases in relative RI, when EPS was present, increased the forward scattering of photons, relative to backward scattering or reflectance by up to ~10%–15%. Observations of natural mat sediments, compared with no-mat sediments, using BDRF showed an increase in forward scattering due to the presence of a mat (Fig. 6).

*Sediment porosity*—The porosity of sediments within a sampling area was greatest in the upper 2 mm of sediment (Fig. 7). Porosity values, expressed as *F* and estimated from resistivity, ranged from 0.4 to 0.8. The presence of a mat revealed an increase in porosity values at a given depth, compared with sediments of an adjacent no-mat area, to a depth of ~10 mm.

## Discussion

Decreases in spectral reflectance were observed from marine carbonate sediments containing microbial mats, compared with similar no-mat sediments. Results of experimental manipulations of sediments showed that the presence of a mat increased the absorption and downward penetration of incident light into sediments across a broad spectral range, a process that was strongly influenced the presence of EPS of mat microorganisms. A range of detailed studies have been conducted in the past that have used optical microprobes to examine the light fields of microbial mats (Jørgensen and Des Marais 1986, 1988; Lassen et al. 1992; Kühl and Jørgensen 1994; Kühl et al. 1994*a,b*, 1996, 1997).
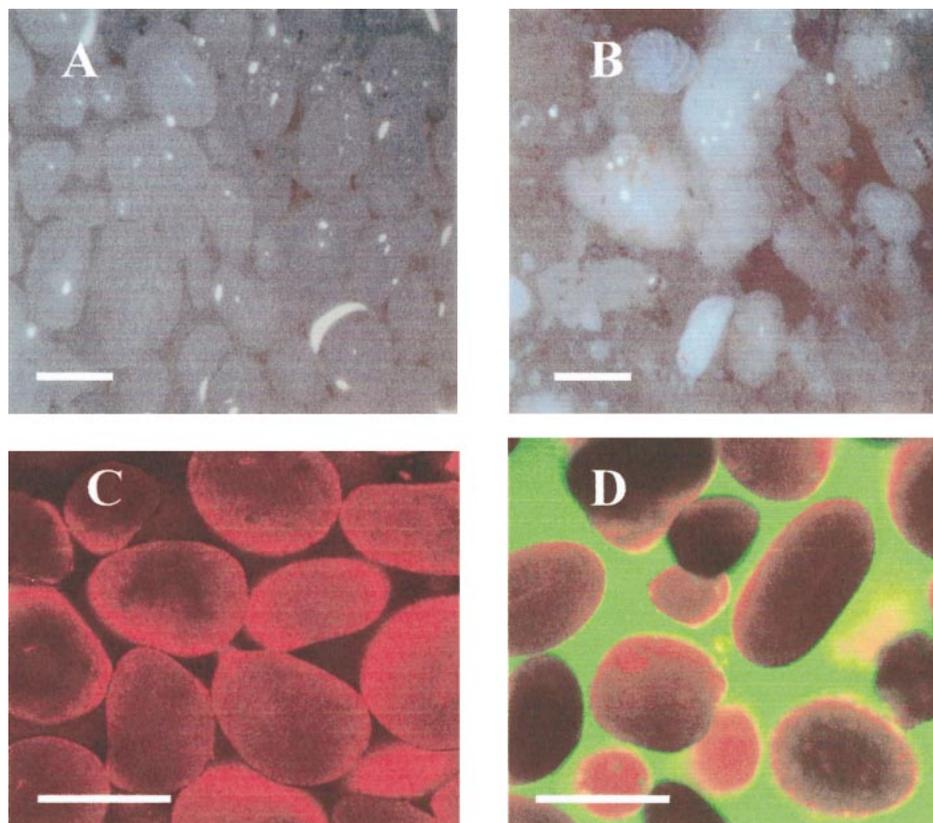
Fig. 4. Light micrographs showing (A) no-mat and (B) mat surface sediments from TB. Note the close packing of sediment grains in the no-mat sample and the relative spreading and suspension of sediment particles within the EPS gel matrix (not visible) in the mat area sample. Confocal laser scanning microscope section of experimental sediments containing (C) no EPS and (D) added EPS-coated sediment. Note the close packing of sediment (ooid) grains (red autofluorescence) in the no-mat section, versus relative spacing of grains when EPS (FITC green autofluorescence) is present. Scale bars, 100 $\mu$m.

Many of these studies have shown that near-surface light fields within sediments are often highly diffuse. This implies that photosynthetic cells probably collect incident light from all directions (Kühl and Jørgensen 1994; Kühl et al. 1994b). Our data suggest that the forward-scattering properties inherent to the EPS gel matrix of mats may strongly contribute to this process.

Sediment grain-size distributions were similar between mat areas and no-mat areas within a given site (Reid 1998), however, were variable between sites (Table 1). Intensive sampling and the results of subsequent laboratory analyses showed that the surface sediments of these sites contained large differences in photosynthetic pigments, EPS abundance, and sediment porosity.

A well-developed microbial mat imparts substantial structural properties to the sediment fabric (Paterson 2001). This results from the interactions of mineral grains, microbial cells, and the EPS matrix. Although biofilms occur on virtually all marine sediment particles, the relative abundances of cells and EPS vary along a continuum ranging from relatively clean sediment having low biomass to well-developed microbial mats where sediment microstructure has been strongly influenced by biogenic processes (Paterson 2001).

The mat and no-mat areas sampled in our study sites were chosen as relative "extremes" along this continuum. The no-mat areas likely represented sediments following a recent physical or biological disturbance. Therefore, our designated no-mat areas contained relatively low amounts of (similar) pigments and EPS compared with adjacent mat areas. The three sediment sites, TB, NP, and OS, were chosen for their obvious patchiness over meter scales in sedimentary characteristics. The TB and NP sites contained surface sediments having clearly visible (i.e., using SCUBA) microbial mats (mat sediments) with interspersed adjacent bare sand patches (no-mat areas). When examined by specific pigment concentrations (Table 2), TB mat areas had five times higher concentrations of pigments compared with their no-mat counterparts. Periodic observations by one of us (R.W.) suggested that mats begin forming on recently disturbed sediments and develop into mat areas over periods of weeks to months.

Ultimately, the distinctly diverse characteristics, in terms of biomass and composition of sediment biofilms at the different sampling sites, were largely responsible for significant variations in hyperspectral reflectance measured at the sediment surface. Reflectance spectra varied in shape because

## Upwelling irradiance (% of surface)
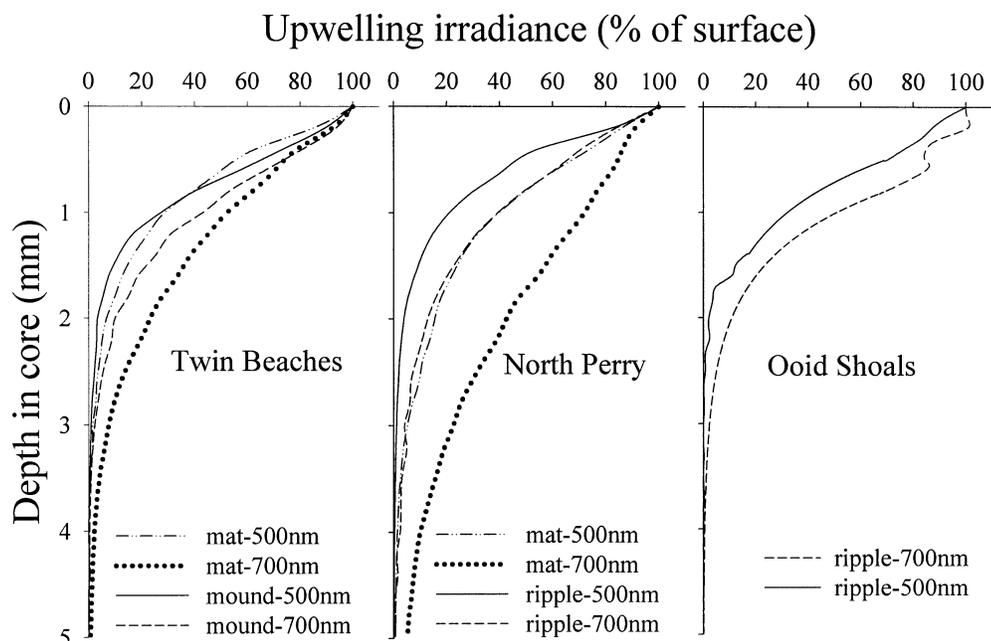


Fig. 5. Plot of light penetration depth relative to levels measured at the sediment surface for all three study sites in April 2001 using the fiber-optic microprobes. Each plotted curve is an average of 3–6 measured profiles from a single core measured at 0.1-mm intervals down-core. In both sites where mats are found (NP and TB), the depth of light penetration was greater than no-mat sands at the same wavelength. The no-mat sediment samples were collected from *Callianassa* mounds at TB and migrating ripples at NP and OS.

of absorption by photosynthetic and photoprotective pigments in microalgal communities.

Sediment sites showed distinct differences in the types of major pigments that were present. The HPLC pigment data, in conjunction with direct microscopic observations, indicated that different phototrophic flora were responsible for the microbial communities at the TB, NP, and OS sites. Pigment patterns within a given site, however, were generally similar between mat and no-mat areas (Table 2). Relatively high concentrations of fucoxanthin relative to other taxo-
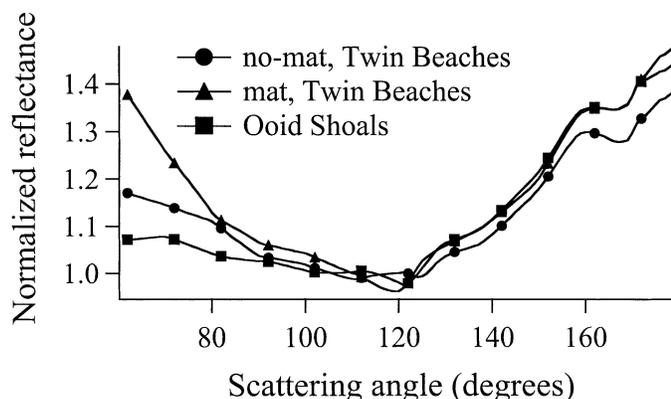


Fig. 6. Normalized BRDF factor along principle plane versus scattering angle. Incident angle for light was 55°, measurement at 640 nm. Three samples are shown: OS and two TB samples, mat and no-mat sediments. The graph illustrates larger forward scattering by the TB mat area sediments, relative to the TB no-mat area.

nomically significant accessory pigments (Wiltshire et al. 1996) indicated that diatoms were a major component of the microbial communities at the NP site both in mat and no-mat areas. The general lower abundance of pigments (and lack of thick mats) of no-mat areas suggested that these bare sand patches may represent areas where a recent physical/biological disturbance of mats may have recently occurred. Reflectance was highest at the no-mat areas of the TB site and at the OS site. The lowest reflectance measured was at the NP site with a thick biofilm which consisted of the highest microalgal pigment biomass as well as a significant amount of EPS. Sediments at the NP site also had the largest mean grain size, a property that may have influenced (i.e., decreased) spectral reflectance, relative to other sites. Although pigments were responsible for changes in the shape of the reflectance spectra, our laboratory studies examining the specific effects of EPS indicated that EPS coatings on bleached sediments can contribute to as much as a 25% decrease in the magnitude of reflectance from 400 to 750 nm.

All samples, at all sites, could not be collected at the same time, nor day, because of the logistical distances between sample sites and time involved in the processing of samples. All samples were subtidal and collected during midday. Therefore, it is possible that the high light conditions may have resulted in the downward migration of photosynthetic cells into the mat. Such migrations have been noted in the past (Bebout and Garcia-Pichel 1995; Serodio et al. 1997; Paterson et al. 1998; Underwood et al. 1999). We did not distinguish the vertical migration of cells in our study. In some samples, however, there were high pigment concentra-
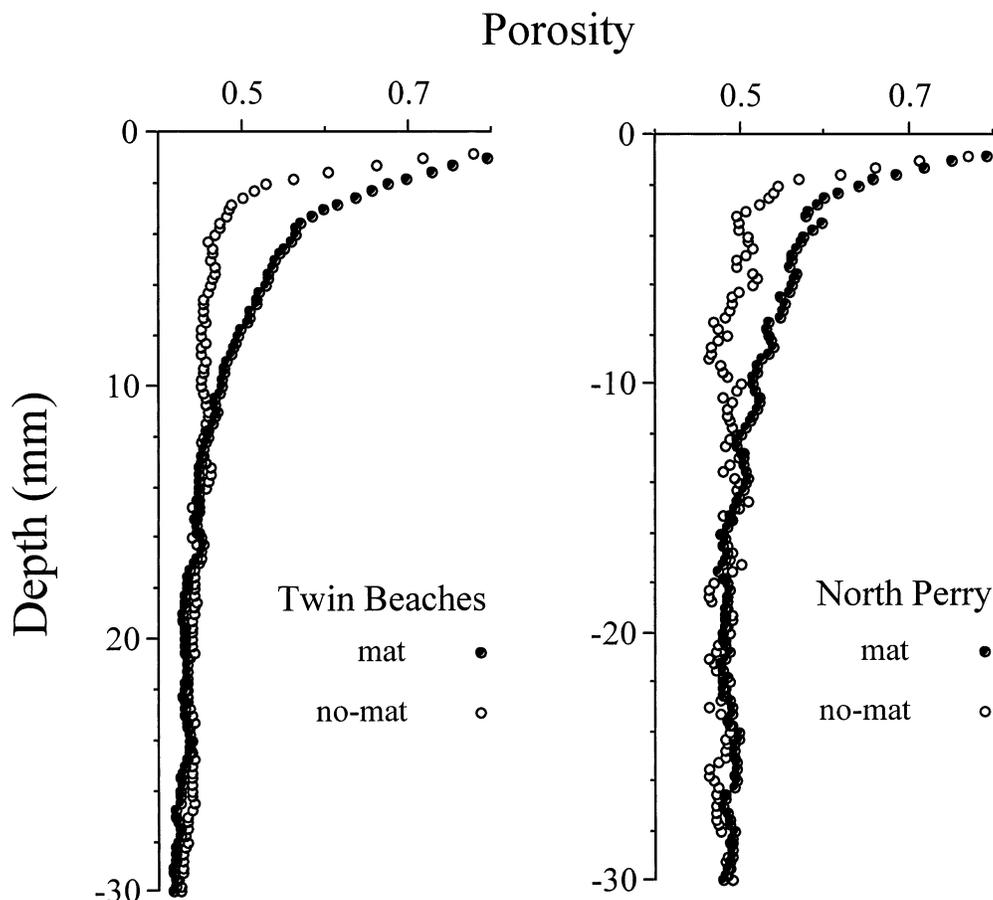
## Porosity



Fig. 7.   Mean (*n* = 6) porosity profiles for mat and no-mat sediments measured with the in situ resistivity profiler at TB and NP in April 2001. The SD for most depth increments is ±0.03.

tions, while relatively low reflectance absorptions (for pigments) were observed. It is possible, therefore, that such downward migrations of cells may have resulted in the relatively low reflectance absorptions near pigment peaks in the reflectance spectra of some mat samples. Also, because analytical measurements often required the disruption/destruction of samples, separate samples had to be used for many measurements. Therefore, we assumed that samples within a given mat or no-mat area, within a site, were relatively homogeneous. This assumption was supported by the relatively low standard errors derived from replicates within an area/measurement (see below).

Natural EPS is highly variable in its chemical composition and likely exists in a continuum of partial degradation states (Decho 1990). The relatively translucent properties of EPS suggest that it may act as an ''optical lens'' that alters the absorption, reflectance, and scattering of light by sediments. Our studies used alginate as an optical ''model'' for EPS owing to the translucent nature of this EPS and it ability to form gels through bidentate complexing in the presence of $Ca^{2+}$ ions, a process that many natural EPS are thought to use (Sutherland 1990). The absorption properties of alginate (Fig. 2) were similar to those of natural EPS isolated from the TB and NP sites. Our measurements (Fig. 2) showed that EPS was not highly absorptive over most of the visible light

spectrum (i.e., 400–700 nm). EPS isolated from mats at NP and TB and laboratory alginate showed similar absorption spectra (Fig. 2). These data suggest that, at the maximum absorbance wavelengths for Chl *a,* the EPS forms a relatively translucent matrix for efficiently transferring photons to potential photopigments. Relative absorption increased in a concentration-dependent manner, over the concentration range of most observed EPS (0.5–4.0 wt%, data not shown). We do not imply that Na-alginate is representative of all EPS in nature. It appears, given our data, however, that EPS matrix represents a relatively translucent medium for transmitting (visible-wavelength) photons to photosynthetic cells.

EPS are important structuring agents of microbial mats and many sediment systems (Underwood et al. 1995; de Winder et al. 1999) and may contribute to the physical stability of mat area sediments. EPS abundance in surface (0–5 mm depth) sediments varied dramatically between mat and no-mat areas within a site and between sites and was closely associated with the presence of mat-forming photosynthetic cells. The contents of EPS ($\mu$g g$^{-1}$ dry sediment) were consistently higher in mat sediments, when compared with adjacent no-mat sediments within a given sample site (Fig. 1). This pattern was consistent across all sample sites. The highest mean (±SE; *n* = 3) EPS content occurred at mat areas of the TB site (274 ± 16 $\mu$g EPS g$^{-1}$ sediment). Some in-

vestigators (Staats et al. 2000) have found higher contents (up to 5,000 $\mu$g EPS g$^{-1}$ sediment) in muddy sediments. Therefore, the mat areas sampled in our study do not represent the most EPS-rich sediments. At both the NP and TB sites, the EPS abundance was ~10–20-fold higher in mat areas compared with adjacent no-mat areas (Fig 1). The mean hexose-equivalent (polysaccharide) content of EPS isolated from mat sediments, as measured by the phenol-sulfuric acid method, was 33 $\pm$ 1.1 wt% and 11.2 $\pm$ 1.1% at no-mat areas of the TB site. NP mat sediments had a mean hexose-equivalent content of 13.7 $\pm$ 0.9%. This suggested that a large portion of the extractable EPS was not composed of hexose sugars that could be hydrolyzed using the phenol-sulfuric acid method (Dubois et al. 1956). The absence of absorption peaks near 280 nm, however, suggested that this EPS material was not protein containing the amino acids tryptophan, tyrosine, and phenylalanine (Scopes 1994).

EPS concentrations in natural surface sediments may be highly variable over small spatial scales (e.g., $\mu$m to cm) (Decho 2000). Gellike aggregates were a frequent occurrence in the surface sediment texture of surface sediments of mat areas at both the TB and NP sites. The ability of the gel matrix to separate sediment grains, increasing the relative spacing of grains (Fig. 4) when compared with sediments in adjacent no-mat areas, was apparent using light and confocal laser microscopy. Similar changes in sediment grain spacing (and resulting spectral reflectance) were achieved using experimental sediments having 4% EPS concentrations.

The surfaces of intact sediment cores of mat sediments exhibited major decreases in reflectance at both 444 and 678 nm that could be attributed to absorption by photopigments, primarily Chl *a,* present in cells. Examinations of reflectance spectra from mat sediments also revealed relatively uniform decreases in reflectance across a wide spectral range (i.e., 400–700 nm) that could not be attributed to spectral absorbance by cells and/or their associated photopigments.

EPS may additionally affect the reflectance by increasing sediment grain spacing. The presence of a dense EPS gel matrix altered grain spacing between ooids. This was obvious in natural sediments and in experimental sediments to which EPS was artificially added. Although sediment grain-size distributions varied between the different sites, they were similar within a given site. Measurements between mat and no-mat sediments, within a sample site showed that grain-size distributions were similar, and thus the observed changes in spectral reflectance between mat and no-mat sediment could not have been due to changes in grain size. However, microscope (light and confocal laser scanning) observations (Fig. 4) showed the presence of abundant EPS gels in the surface sediments that were collected from mat areas. Sediment porosity (Fig. 7) was typically higher in mat sediments, as measured by an in situ resistivity profiler device (Wheatcroft in press). Other studies (de Winder and Stal 1997; Noffke et al. 2001) found that the presence of microbial mats was associated with an increased porosity of sediments, extending down to ~10 mm depth, a conclusion similar to our own study (Fig. 7). The presence of cyanobacterial films on sediments altered the bedding structure, including the pore-water fabrics, of sediments. These changes are often so significant that they proposed that microbially mediated

structures be a fifth category in the existing classification scheme of primary sediment structures.

In our study, differences in grain sizes between sites may have accounted for variability in reflectance between sites (e.g., NP vs. TB, Fig. 3). The slightly higher mean grain size at NP may be a minor factor influencing the lower magnitudes of reflectance, relative to TB, although penetration depths of light in no-mat areas at all three sediment sites were similar (Fig. 5). The increased porosity and light-altering capabilities of the mat matrix likely explains the increased light penetration observed in the mat samples at NP and TB, relative to no-mat sediment from the same site. On average, the depth to 10% incident light was 20%–80% deeper, depending on wavelength, in mat covered areas. The much larger increases observed at NP relative to the TB mats is likely a function of the more advanced stage of development, leading to higher porosities and increased EPS content.

Previous work (Jørgensen and Des Marais 1986, 1988; Kühl and Jørgensen 1992; Lassen et al. 1992; Kühl et al. 1994*a,b*) has shown that the light fields within sediments can be quite diffuse, because of strong multidirectional scattering. It is important to note that a flat-tip (compared with a spherical tip) fiber-optic microprobe was used in the present study. Previous studies (Kühl et al. 1994*a*; Fukshansky-Kazarinova et al. 1996; Holst et al. 2000) have shown that a spherical probe tip collects incident light isotropically and thus provides a better measure of light within sediment environments. Therefore, our measurements of light penetration with sediment depth (Fig. 5) should be considered ''conservative'' ones. The large differences observed between mat and no-mat sediments, however, strongly suggests that light penetration is greater in sediments containing surface microbial mats.

Results of laboratory experiments showed that sediments having higher EPS concentrations exhibited increased forward scattering relative to no-EPS sediments (Fig. 3B). The presence of an EPS gel around a sand gain reduced the relative index of refraction of the grain, compared with a similar grain in seawater. The decrease in relative RI, when EPS was present, increased the forward scattering of photons, relative to backward scattering or reflectance, by up to 10%–15%. Observations of natural mat sediments, compared with no-mat sediments, using BDRF showed an increase in forward scattering due to the presence of a mat (Fig. 6). Reflectance, therefore, may have decreased from a combination of increased absorption around ooid grains, along with the change in index of refraction. The index of refraction change increased the amount of forward scatter relative to backscatter and thus increased the penetration of light into the sediment (in addition to grain spacing effects).

Laboratory manipulations of sediments were designed to specifically investigate the potential effects of EPS on sediment reflectance spectra. The results of these experiments showed that a ~20%–30% decrease in reflectance could be observed compared with no-EPS (control) sediments, over a wide spectral range (400–700 nm). At 2% and 4% (wt/vol) concentrations, EPS formed coherent gels that successfully spaced sediment grains apart from each other, compared with no-EPS controls. The reflectance decrease, however, became most pronounced at the highest EPS concentration (i.e., 4%).

Light penetration to 10% incident is 80% deeper in the 2% EPS and 262% deeper in the 4% EPS relative to the non-EPS controls.

We purposefully used precleaned and presieved carbonate ooids in our experimental studies, to control potential sedimentological and organic matter effects, so that specific EPS effects could be examined. Thus, we did not determine how larger (or smaller) sediment grain sizes and/or shape may influence the reflectance and scattering spectra of sediments. Natural ooids, even after cleaning with sodium hypochlorite, still contained traces of chlorophyll and other pigments that were detectable in reflectance spectra. This was likely due to the presence of endolithic cyanobacteria that are sealed within sediment ooids. These endoliths are typical of many ooid environments in the Bahamas (Macintyre et al. 2000 and citations within).

Microbial EPS may change the relative index of refraction of the particles that it is surrounding. This will reduce reflectance, by enhancing forward scattering (Twomey et al. 1986), but might additionally have the effect of increasing penetration into sediment. It was concluded from these data that the EPS matrix, when present in sufficient quantities, may reduce the spectral reflectance of surface sediments. This occurred through two different, but co-occurring, mechanisms: (1) by changing the relative spacing of sand grains, a process that altered the amount of light entering sediments, and (2) by effecting the forward scattering of photons through EPS. It is likely that the relatively large molecular size, rather than specific compositional moieties, of EPS molecules contribute to its (forward scattering) properties, and overall effects on spectral reflectance. If that were the case, then biofilms produced by heterotrophic communities should also exhibit these properties.

*Implications*—The biofilm gel effect has several important functional implications for surface-associated microbial photosynthesis. Our data suggest that the biofilm gel effect in sediments acts to trap photons more efficiently than sediments alone. The enhanced forward scattering, in conjunction with the increased porosity (i.e., spreading of sediment grains) would allow down-welling photons to penetrate deeper into the sediments and hence would allow photosynthesis to occur at greater relative depths. Dense layers of photosynthetic cells that often occur in mat layers, if immediately surrounded by EPS gels, would be potentially less subject to shading effects by overlying cells. Additionally, the EPS gel would allow the ''recapture'' of reflected or scattered photons from an underlying surface and thus increase the chances of absorption by cellular chromophores. The biofilm gel effect, therefore, should influence the ability of sediment-associated and densely packed photosynthetic microbial cells to acquire solar energy. Over broader spatial scales, the EPS gel matrix of biofilms may influence photon processing at the Earth's surface.

## References

AMOS, C. L., T. F. SUTHERLAND, B. RADZIJEWSKI, AND M. DOUCETTE. 1996. A rapid technique to determine bulk density of fine-grained sediments by x-ray computed topography. J. Sed. Res. **66:** 1023–1025.

ARCHIE, G. E. 1942. The electrical resistivity log as an aid in determining some reservoir characteristics. Trans. Am. Inst. Mining Metallurg. Eng. **146:** 54–62.

BEBOUT, B. M., AND F. GARCIA-PICHEL. 1995. UVB-induced vertical migration of cyanobacteria in a microbial mat. Appl. Environ. Microbiol. **61:** 4215–4222.

COSTERTON, J. W., Z. LEWANDOWSKI, D. E. CALDWELL, D. R. KORBER, AND H. M. LAPPIN-SCOTT. 1995. Microbial biofilms. Annu. Rev. Microbiol. **49:** 711–45.

DECHO, A. W. 1990. Microbial exopolymer secretions in ocean environments: Their role(s) in food webs and marine processes. Oceanogr. Mar. Biol. Annu. Rev. **28:** 73–153.

———. 2000. Microbial biofilms in intertidal systems. Cont. Shelf Res. **20:** 1257–1273.

———, AND T. KAWAGUCHI. 1999. Confocal imaging of in-situ natural microbial communities and their extracellular polymeric secretions using Nanoplast resin. BioTechniques **27:** 1246–1252.

———, AND ———. 2000. Biochemical characterization of cyanobacterial extracellular polymers (EPS) from Bahamas. Prep. Biochem. Biotechnol. **30:** 321–330.

DE WINDER, B., N. STAATS, L. J. STAL, AND D. M. PATERSON. 1999. Carbohydrate secretion by phototrophic communities in tidal sediments. J. Sea Res. **42:** 131–146.

———, AND L. J. STAL. 1997. Measurements of resistivity in the Eden estuary. *In* D. M. Paterson, L. Stal, and W. E. Krumbein [eds.], Primary productivity and microbially-mediated transport of elements (C, P, Fe) in tide-influenced deposits. Project EV5V-CT94-0411, final report, EU MAST Programme.

DUBOIS, M., K. A. GILLES, J. K. HAMILTON, P. A. REBER, AND F. SMITH. 1956. Colorimetric method for determination of sugars and related substances. Anal. Chem. **28:** 350–356.

FUKSHANSKY-KAZARINOVA, N., L. FUKSHANSKY, M. KÜHL, AND B. B. JØRGENSEN. 1996. Theory of equidistant three-dimensional radiance measurements with optical microprobes. Appl. Optics **35:** 65–73.

HAY, S. I., T. C. MAITLAND, AND D. M. PATERSON. 1993. The speed of diatom migration through natural and artificial substrata. Diatom Res. **8:** 371–384.

HOLST, G., I. KLIMAT, O. KOHLS, AND M. KÜHL. 2000. Optical microsensors and microprobes, p. 143–148. *In* M. Varney [ed.], Chemical sensors in oceanography. Gordon and Breach.

JØRGENSEN, B. B., AND D. J. DES MARAIS. 1986. A simple fiber-optic microprobe for high resolution light measurements: Application in marine sediment. Limnol. Oceanogr. **31:** 1376–1383.

———, AND ———. 1988. Optical properties of benthic photosynthetic communities: Fiber-optic studies of cyanobacterial mats. Limnol. Oceanogr. **33:** 99–113.

KÜHL, M., R. N. GLUD, H. PLOUG, AND N. B. RAMSING. 1996. Microenvironmental control of photosynthesis and photosynthesis-coupled respiration in an epilithic cyanobacterial biofilm. J. Phycol. **32:** 799–812.

———, AND B. B. JØRGENSEN. 1992. Spectral light measurements in microbenthic phototrophic communities with a fiber-optic microprobe coupled to a sensitive diode array detector. Limnol. Oceanogr. **37:** 1813–1823.

———, AND ———. 1994. The light field of microbenthic communities: Radiance distribution and microscale optics of sandy coastal sediments. Limnol. Oceanogr. **39:** 1368–1398.

———, C. LASSEN, AND B. B. JØRGENSEN. 1994a. Light penetration and light intensity in sandy marine sediments measured with irradiance and scalar irradiance fiber-optic microprobes. Mar. Ecol. Prog. Ser. **105:** 139–148.

————, ————, AND ————. 1994*b*. Optical properties of microbial mats: light measurements with fiber-optic microprobes, p. 149–166. *In* L. J. Stal and P. Caumette [eds.], Microbial mats: Structure, development and environmental significance. NATO ASI series 35. Springer-Verlag.

————, ————, AND N. P. REVSBECH. 1997. A simple light meter for measurements of PAR (400 to 700 nm) with fiber-optic microprobes: Application for P vs. $E_0$ (PAR) measurements in a microbial mat. Aquat. Microb. Ecol. **13:** 197–207.

LASSEN, C., H. PLOUG, AND B. B. JØRGENSEN. 1992. A fibre-optic scalar irradiance microsensor: Application for spectral light measurements in sediments. FEMS Microbiol. Ecol. **86:** 247–254.

MACINTYRE, I. G., L. PRUFERT-BEBOUT, AND R. P. REID. 2000. The role of endolithic cyanobacteria in the formation of lithified laminae in Bahamian stromatolites. Sedimentology **47:** 915–921.

MOBLEY, C. D. 1994. Light and water: Radiative transfer in natural waters. Academic.

NOFFKE, N., G. GERDES, T. KLENKE, AND W. E. KRUMBEIN. 2001. Microbially induced sedimentary structures—a new category with the classification of primary sedimentary structures. J. Sed. Res. **71:** 649–656.

PATERSON, D. M. 1995. The biogenic structure of early sediment fabric visualized by low-temperature scanning electron microscopy. J. Geol. Soc. **152:** 131–140.

————. 2001. The fine structure and properties of the sediment surface, p. 127–143. *In* B. P. Boudreau and B. B. Jørgensen [eds.], The benthic boundary layer: Transport processes and biogeochemistry. Oxford University Press.

————, AND OTHERS. 1998. Microbial mediation of spectral reflectance from intertidal cohesive sediments. Limnol. Oceanogr. **43:** 1207–1221.

PHILPOT, W. D. 1989. Bathymetric mapping with passive multispectral imagery. Appl. Optics **28:** 1569–1578.

PINCKNEY, J. L., D. F. MILLIE, K. E. HOWE, H. W. PAERL, AND J. P. HURLEY. 1996. Flow scintillation counting of 14C-labeled microalgal photosynthetic pigments. J. Plankton Res. **18:** 1867–1880.

REID, R. P. 1998. Composition, texture and diagenesis of carbonate sediments: Effects on benthic optical properties. Office of Naval Research Ocean Atmosphere and Space.

SCOPES, R. K. 1994. Protein purification: Principles and practice, 3rd ed. Springer-Verlag.

SERODIO, J., J. M. DA SILVA, AND F. CATARINO. 1997. Non-destructive tracing of migratory rhythms of intertidal benthic microalgae using in vivo chlorophyll a fluorescence. J. Phycol. **33:** 542–553.

SMITH, D. J., AND G. J. C. UNDERWOOD. 1998. Exopolymer production by intertidal epipelic diatoms. Limnol. Oceanogr. **43:** 1578–1591.

STAATS, N., L. J. STAL, B. DE WINDER, AND L. R. MUIR. 2000. Oxygenic photosynthesis as a driving process in exopolysaccharide production in benthic diatoms. Mar. Ecol. Prog. Ser. **193:** 261–269.

SUTHERLAND, I. W. 1990. Biotechnology of microbial exopolysaccharides. Cambridge University Press.

SUTHERLAND, T. F. 1996. Biostabilization of estuarine subtidal sediments. Ph.D. dissertation, Dalhousie University.

TWOMEY, S. E., C. F. BOHREN, AND J. L. MERGENTHALER. 1986. Reflectance and albedo differences between wet and dry surfaces. Appl. Optics **25:** 431–437.

UNDERWOOD, G. J. C., C. NILSSON, K. SUNDBÄCK, AND A. WULFF. 1999. Short-term effects of UV-B radiation on chlorophyll fluorescence, biomass, pigments and carbohydrate fractions in a benthic diatom mat. J. Phycol. **35:** 656–666.

————, D. M. PATERSON, AND R. J. PARKES. 1995. The measurement of microbial carbohydrate exopolymers from intertidal sediments. Limnol. Oceanogr. **40:** 1243–1253.

VAN HEUKELEM, L., A. J. LEWITUS, T. M. KANA, AND N. E. CRAFT. 1994. Improved separations of phytoplankton pigments using temperature-controlled high performance liquid chromatography. Mar. Ecol. Prog. Ser. **114:** 303–313.

VOSS, K. J., A. CHAPIN, M. MONTI, AND H. ZHANG. 2000. An instrument to measure the bi-directional reflectance distribution function (BRDF) of surfaces. Appl. Optics **39:** 6197–6206.

WHEATCROFT, R. A. In press. In situ measurements of near-surface porosity in shallow-marine sands. IEEE J. Ocean Engin.

WILTSHIRE, K. H., C. D. GEISSLER, F. SCHROEDER, AND H. D. KNAUTH. 1996. Pigments in suspended matter from the Elbe estuary and the German Bight. Their use as marker compounds for the characterization of suspended matter and in the interpretation of heavy metal loadings. Arch. Hydrobiol. Spec. Iss. Adv. Limnol. **47:** 53–63.

YATES, M. G., A. R. JONES, S. McGRORTY, AND J. D. GOSS-CUSTARD. 1993. The use of satellite imagery to determine the distribution of intertidal surface sediments of the Wash, England. Estuar. Coast. Shelf Sci. **36:** 333–344.